Available online at www.sciencedirect.com
ScienceDirect
Journal of Sound and Vibration 303 (2007) 723–740
JOURNAL OF SOUND AND VIBRATION
www.elsevier.com/locate/jsvi

Free vibration of a beam subjected to large static deflection

Marie-Blanche Cornil[a], Laurent Capolungo[a], Jianmin Qu[a,*], Vivek A. Jairazbhoy[b]

[a]*School of Mechanical Engineering, Georgia Institute of Technology, Atlanta, GA 30332-0405, USA*
[b]*Advanced Technology Development, Visteon Corporation, Dearborn, MI 48121, USA*

Received 5 March 2007; accepted 1 February 2007
Available online 5 April 2007

Abstract

Considered in this paper is the problem of free vibration of a beam that has undergone a large static deflection. The nonlinear equations of motion for the beam are derived first. The equations are then decomposed into a set of nonlinear differential equations for the static deflection and a set of linear differential equations for the vibrational motion of the beam. The coefficients of the vibration equations consist of the beam's static deflection. The nonlinear differential equations are solved analytically to obtain the static deflection. The vibration equations are solved by expanding the displacements in a power series. Coefficients of the power series are constructed analytically through a recursive relationship. The natural frequencies of the beam under large static bending are determined by solving a 3×3 eigenvalue problem. Substitution of the eigenvalues and eigenvectors into the power-series expansion of the displacements yields the corresponding modes of vibration. Several numerical examples are given to illustrate the solution procedure.

1. Introduction

In a number of emerging technical areas, there is a need to bend thin plates (beams) into various shapes. For example, optical fibers are used in various communication cables. To have high reliability and performance, deformation of the thin optical fibers near the optical/electrical connectors must be considered. In the electronic packaging area, more and more flexible circuit boards are being used for small, light and high performance electronic products [1–3]. Surface-mount-device-on-flex, chip-on-flex and flip-chip-on-flex are becoming commercially mature technologies. However, the compliant nature of the flexible circuit board poses significant technical challenges to the standard surface mount technology. One of the issues is the vibration of such flexible circuits. The resonant vibration causes damage to the components on the board and produces undesirable noise. To develop techniques for vibration control, dynamic characteristics of such flexible circuit boards must be understood when they are subjected to large static deflection. This calls for the study of vibration of plates and beams subjected to large static deflection.

Based on the classical Kirchhoff theory [4], vibrations of straight beams and flat plates are well understood. The vibration of curved beams, rings and arches has also been the subject of numerous investigations. For example, Chen [5], Petyt and Fleischer [6], and Markus and Nanasi [7] studied the free vibration of curved

*Corresponding author. Tel.: +1 404 894 5687; fax: +1 404 894 0186.
E-mail address: jianmin.qu@me.gatech.edu (J. Qu).

0022-460X/$ - see front matter © 2007 Elsevier Ltd. All rights reserved.
doi:10.1016/j.jsv.2007.02.016

beams; Suzuki and Ishiyama [8] investigated the free vibration of curved bars; Laura and Maurizi [9] developed techniques to analyze the vibration of arch-type structures. In a review paper by Chidamparam and Leissa [10], the existing results for arches, circular and non-circular rings are summarized. Examples of recent work in this area include the study of vibration of beams and helices with arbitrarily large uniform curvature by Tarnopolskaya et al. [11], and the papers by Tseng and Lin on in-plan vibration of arches with variable curvature [12,13].

Although there is a large body of literature on the vibration of curved beams, rings and arches, in these studies it was assumed that the structure (beams, rings, arches) is free of stress in the initial stage (the equilibrium configuration). The only stress induced in the structure is due to vibration. Such an assumption is valid for many structural applications. However, there is a class of applications, such as the flexible printed circuit boards (PCB) mentioned earlier, where the vibration is superimposed on a statically deformed structure. Therefore, the vibration characteristics of the structure are strongly influenced by the existing stress induced by the static deformation. This effect becomes even more pronounced if the static deformation is large. Unfortunately, studies on the vibrational motion of a beam subjected to large static deformation do not seem to exist.

In this paper, we focus on the free vibration of a beam subjected to a large static deflection. The general equations of motion for such a beam are derived first. Under the assumption that the amplitude of vibration is much smaller than the static deflection, the nonlinear equations of motion are decomposed into a set of nonlinear differential equations for the static deformation and a set of linear differential equations for the vibration. The coefficients of the linear vibration equations involve the solution to the nonlinear static equation, which are solved by using the method developed in Xue et al. [14]. The linear vibration equations are expressed in terms of the local displacements in the directions that are axial and transverse to the statically deformed beam. By expanding the displacements in a power series of the Lagrange coordinates along the initial beam length, solutions to the linear vibration equations are obtained. Coefficients of the power series can be constructed recursively once the initial conditions are given. The natural frequencies are determined through a 3×3 eigenvalue problem that depends on the type of boundary conditions.

Flexible PCB are typically attached to the casing of the electronic system either by fasteners or sockets. A commonly encountered configuration is a flexible printed circuit board with each end plugged into a socket affixed to the casing. The sockets are typically not on the same plane. This induces static bending of the printed circuit board. To prevent damage to the on-board circuits and electronic components, the positions and the length of the printed circuit board are designed such that it is not being structured when installed. This situation is idealized into a cantilever beam subjected to a prescribed deflection and rotation at its "free" end, as schematically illustrated in Fig. 1. Using the general solution method derived in the first part of this paper, this problem is solved numerically. Solutions that yield the first three natural frequencies and the corresponding vibration modes are presented. The veering phenomenon [15–17], first observed in the vibration modes of plates and membranes [15], where two natural frequencies become very close at certain point (or over certain region), but never cross over each other while the corresponding vibration modes change drastically near the veering loci, was found to occur at certain specific shapes of the static deformation. Comparisons are made between statically deformed beams and naturally curved beams that have the same initial shape.

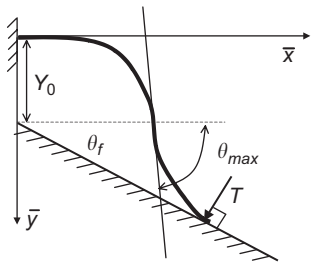

Fig. 1. A cantilever beam with prescribed deflection and rotation at its "free" end.

2. Equations of motion

With reference to Fig. 2 first, consider a fixed Cartesian coordinate system $(\bar{x}, \bar{y})$. The position of a generic point on the neutral axis of the beam can then be indicated by its coordinates. Let (X, Y) be the coordinates of a point on the neutral axis of the beam in the initial (undeformed) state. Assume that, after deformation, this same point has moved to a new location with coordinates (x, y). If S is used to represent the arc-length of the neutral axis of the beam in the initial state, then, these two sets of coordinates are related by

$$x(S,t) = X(S) + u(S,t), \quad y(S,t) = Y(S) + v(S,t), \tag{1}$$

where u and v are the displacement components in the $\bar{x}$-direction and the $\bar{y}$-direction, respectively. Obviously, for an initially straight beam, the undeformed neutral axis of the beam is described by $X = S$ and $Y = 0$.

Next, assume that the beam is subjected to a system of distributed loads q_x, q_y and m. Here, q_x and q_y are in the $\bar{x}$ and the $\bar{y}$ direction, respectively, with the dimension of force per unit length of the beam's neutral axis in the initial state, while m is the moment per unit length of the beam's neutral axis in the initial state.

In addition to the applied loads, the inertial forces in the $\bar{x}$ and the $\bar{y}$ directions are given, respectively, by

$$-\rho A \frac{\partial^2 x(S,t)}{\partial t^2} \mathrm{d}S, \quad -\rho A \frac{\partial^2 y(S,t)}{\partial t^2} \mathrm{d}S. \tag{2}$$

The inertial moment is given by

$$-\rho A J \frac{\partial^2 \theta(S,t)}{\partial t^2} \mathrm{d}S. \tag{3}$$

In Eqs. (2) and (3), ρ is the mass density per unit (initial) volume, A the cross-section area, and J the moment of inertia of the beam cross-section about the neutral axis of the beam. For a rectangular cross-section beam of height h,

$$J = \frac{\mathrm{d}S^2 + h^2}{12} \mathrm{d}S. \tag{4}$$

It is seen that the inertial moment term in Eq. (3) is much smaller than the other terms. In the rest of this paper, it will be neglected.

Equilibrium of all the forces and moments on the element $\mathrm{d}S$ yields

$$\frac{\partial N}{\partial S} = -\rho \frac{\partial^2 x(S,t)}{\partial t^2} - q_x, \quad \frac{\partial V}{\partial S} = \rho \frac{\partial^2 y(S,t)}{\partial t^2} - q_y, \tag{5}$$

$$\frac{\partial M}{\partial S} = -V \frac{\partial x}{\partial S} + N \frac{\partial y}{\partial S}, \tag{6}$$

where N, V and M are, respectively, the components of the internal forces and bending moment as labeled in Fig. 3.

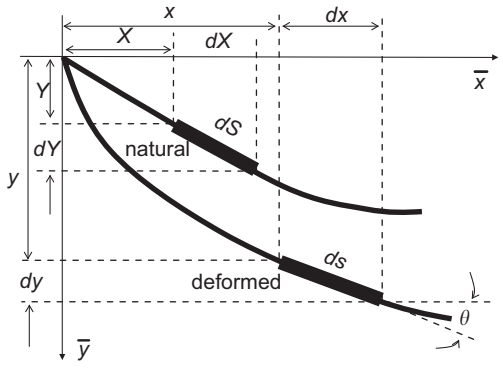

Fig. 2. Deformed and natural configuration of the beam.

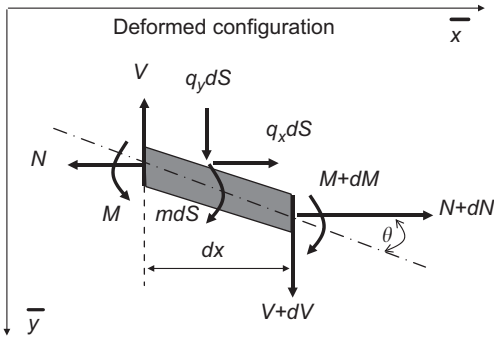

Fig. 3. Free-body diagram of a length element in the deformed configuration.

Deformation of the beam consists of two contributions. One is the axial strain of the neutral axis described by

$$\varepsilon = \frac{\partial s - \partial S}{\partial S} = \frac{\partial s}{\partial S} - 1, \quad \varepsilon = \frac{\mathrm{d}s - \mathrm{d}S}{\mathrm{d}S}. \tag{7}$$

The other contribution comes from the rotation of the beam cross-section described by the angle θ measured from the $\bar{x}$-axis to the neutral axis in the deformed configuration, as shown in Fig. 1. Therefore, a simple geometry analysis in conjunction with Eq. (7) yields the strain and displacement relationships

$$\frac{\partial x}{\partial S} = (1+\varepsilon)\cos\theta, \quad \frac{\partial y}{\partial S} = (1+\varepsilon)\sin\theta. \tag{8}$$

Substituting Eq. (8) into Eq. (6) yields

$$\frac{\partial M}{\partial S} = (1+\varepsilon)(N\sin\theta - V\cos\theta). \tag{9}$$

The constitutive equations that connect the internal forces (N, V, M) and the deformation descriptors (ε,θ) are obtained by using the Hooke's law for linear elastic materials

$$N\cos\theta + V\sin\theta = EA\varepsilon, \quad M = EI\frac{\partial\theta}{\partial S}, \tag{10}$$

where E is the Young's modulus, and I the bending moment of inertia, $I = bh^3/12$ with b being the width and h being the height of the beam.

By combining Eqs. (9) and (10), one can solve for N and V,

$$N = EA\varepsilon\cos\theta + EI\,\frac{\mathrm{d}^2\theta}{\mathrm{d}S^2}\,\frac{\sin\theta}{1+\varepsilon}, \tag{11}$$

$$V = EA\varepsilon\sin\theta - EI\,\frac{\mathrm{d}^2\theta}{\mathrm{d}S}\,\frac{\cos\theta}{1+\varepsilon}. \tag{12}$$

Substitution of Eqs. (11) and (12) into Eq. (5) yields a pair of second-order nonlinear differential equations

$$\frac{\partial}{\partial S}\left\{EA\varepsilon\cos\theta + EI\,\frac{\partial^2\theta}{\partial S^2}\,\frac{\sin\theta}{1+\varepsilon}\right\} = \rho A\,\frac{\partial^2 x}{\partial t^2} - q_x, \tag{13}$$

$$\frac{\partial}{\partial S}\left\{EA\varepsilon\sin\theta - EI\,\frac{\partial^2\theta}{\partial S^2}\,\frac{\cos\theta}{1+\varepsilon}\right\} = \rho A\,\frac{\partial^2 y}{\partial t^2} - q_y. \tag{14}$$

Eqs. (8), (13) and (14) provide a system of four differential equations for the four unknowns, $\varepsilon(S,t)$, $\theta(S,t)$, $x(S,t)$ and $y(S,t)$. These equations are valid for S between 0 and L, the initial (undeformed) beam length.

3. Dynamic solution

To obtain the solution to the vibration problem defined by Eqs. (8), (13) and (14), we represent the solutions to $\varepsilon(S,t)$, $\theta(S,t)$, $x(S,t)$ and $y(S,t)$ by

$$\varepsilon = \varepsilon_0(S) + \varepsilon_1(S,t), \theta = \theta_0(S) + \theta_1(S,t), \tag{15}$$

$$x = x_0(S) + x_1(S,t), y = y_0(S) + y_1(S,t), \tag{16}$$

where the quantities with a subscript 0 are the solution to the static deformation, and the quantities with a subscript 1 represent the small oscillations of the beam in the neighborhood of the static deformation (see Fig. 4). The static deformation was solved by Xue et al. [14]. So, in this paper, we assume that ε_0, θ_0, x_0 and y_0 are known, and will focus on obtaining ε_1, θ_1 x_1 and y_1.

To this end, we first substitute Eqs. (15) and (16) into Eq. (8) to obtain

$$\theta_1 = \frac{1}{1+\varepsilon_0}\left[-\frac{\partial x_1}{\partial s}\sin\theta_0 + \frac{\partial y_1}{\partial s}\cos\theta_0\right], \quad \varepsilon_1 = \frac{\partial x_1}{\partial s}\cos\theta_0 + \frac{\partial y_1}{\partial s}\sin\theta_0. \tag{17}$$

Then, by making use of Eqs. (15) and (17), the equations of motion, Eqs. (13) and (14), can be recast into a pair of fourth-order differential equations for ε_1, θ_1 x_1 and y_1,

$$\begin{aligned}\frac{\partial}{\partial S}\left\{\frac{EI\sin\theta_0}{1+\varepsilon_0}\frac{\partial^2\theta_1}{\partial S^2} + \left[-EA\varepsilon_0\sin\theta_0 + EI\frac{\cos\theta_0}{1+\varepsilon_0}\frac{\mathrm{d}^2\theta_0}{\mathrm{d}S^2}\right]\theta_1\right.\\ \left. + \left[EA\cos\theta_0 - EI\frac{\sin\theta_0}{(1+\varepsilon_0)^2}\frac{\mathrm{d}^2\theta_0}{\mathrm{d}S^2}\right]\varepsilon_1\right\} = \rho A\frac{\partial^2 x_1}{\partial t^2}\end{aligned} \tag{18}$$

and

$$\begin{aligned}\frac{\partial}{\partial S}\left\{-\frac{EI\cos\theta_0}{1+\varepsilon_0}\frac{\partial^2\theta_1}{\partial S^2} + \left[EA\varepsilon_0\cos\theta_0 + EI\frac{\sin\theta_0}{1+\varepsilon_0}\frac{\mathrm{d}^2\theta_0}{\mathrm{d}S^2}\right]\theta_1\right.\\ \left. + \left[EA\sin\theta_0 + EI\frac{\cos\theta_0}{(1+\varepsilon_0)^2}\frac{\mathrm{d}^2\theta_0}{\mathrm{d}S^2}\right]\varepsilon_1\right\} = \rho A\frac{\partial^2 y_1}{\partial t^2}.\end{aligned} \tag{19}$$

Finally, consider the boundary conditions. Since the static solution satisfies the inhomogeneous boundary conditions, the dynamic part of the solution only needs to satisfy the homogeneous boundary conditions

$$x_1(0,t) = y(0,t) = \left.\frac{\partial x_1(s,t)}{\partial s}\right|_{s=0} = \left.\frac{\partial y_1(s,t)}{\partial s}\right|_{s=0} = 0, \tag{20}$$

$$x_1(L,t) = y_1(L,t) = \left.\frac{\partial x_1(s,t)}{\partial s}\right|_{s=L} = \left.\frac{\partial y_1(s,t)}{\partial s}\right|_{s=L} = 0. \tag{21}$$

Eqs. (17)–(19) provide the governing equations and boundary conditions for the four unknowns ε_1, θ_1 x_1 and y_1. To reduce these equations to a form convenient for solution, let us introduce the axial and transverse

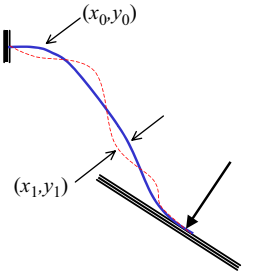

Fig. 4. Small amplitude oscillation about the deformed beam. The solid line is the statically deformed shape of the beam and the dashed line represents the vibration.

displacements u and v, respectively, through

$$u = x_1 \cos\theta_0 + y_1 \sin\theta_0, \quad v = -x_1 \sin\theta_0 + y_1 \cos\theta_0. \tag{22}$$

After some algebra, see Appendix A, we can reduce Eqs. (17)–(19) into a pair of fourth-order differential equations for the displacements u and v,

$$\sum_{n=0}^{2} A_n L^n \frac{\mathrm{d}^n u}{\mathrm{d}S^n} + \sum_{n=0}^{3} B_n L^n \frac{\mathrm{d}^n v}{\mathrm{d}S^n} = \frac{\rho L^2}{E} \frac{\partial^2 u}{\partial t^2}, \tag{23}$$

$$\sum_{n=0}^{4} C_n L^n \frac{\mathrm{d}^n v}{\mathrm{d}S^n} + \sum_{n=0}^{3} D_n L^n \frac{\mathrm{d}^n u}{\mathrm{d}S^n} = \frac{\rho L^2}{E} \frac{\partial^2 v}{\partial t^2}, \tag{24}$$

where the coefficients A_n, B_n, C_n and D_n are functions of the static deflection, as well as the geometry and material properties of the beam. The full expressions are given in Appendix B.

In the case of time-harmonic vibration, one may assume

$$u = \bar{u}(\bar{S})\exp(\mathrm{i}\omega t), \quad v = \bar{v}(\bar{S})\exp(\mathrm{i}\omega t), S = \bar{S}L. \tag{25}$$

Then, Eqs. (23) and (24) can be recast into

$$\sum_{n=0}^{2} A_n \frac{\mathrm{d}^n \bar{u}}{\mathrm{d}\bar{S}^n} + \sum_{n=0}^{3} B_n \frac{\mathrm{d}^n \bar{v}}{\mathrm{d}\bar{S}^n} + \alpha^2 \bar{u} = 0, \tag{26}$$

$$\sum_{n=0}^{4} C_n \frac{\mathrm{d}^n \bar{v}}{\mathrm{d}\bar{S}^n} + \sum_{n=0}^{3} D_n \frac{\mathrm{d}^n \bar{u}}{\mathrm{d}\bar{S}^n} + \alpha^2 \bar{v} = 0, \tag{27}$$

where

$$\alpha^2 = \frac{\rho L^2 \omega^2}{E} \quad \text{or} \quad \omega = \alpha\sqrt{\frac{E}{\rho L^2}}. \tag{28}$$

The boundary conditions are

$$\bar{u}(0) = \bar{v}(0) = \bar{v}'(0) = \bar{u}(1) = \bar{v}(1) = \bar{v}'(1) = 0. \tag{29}$$

4. Numerical solution procedure

In what follows, we develop a numerical method to solve the governing equations, Eqs. (26) and (27) with the boundary condition Eq. (29). The first step is to expand formally the unknown displacements into power series of $\bar{S}$,

$$\bar{u} = \sum_{n=0}^{\infty} \bar{u}_n \bar{S}^n, \quad \bar{v} = \sum_{n=0}^{\infty} \bar{v}_n \bar{S}^n, \tag{30}$$

where $\bar{u}_n$ and $\bar{v}_n$ are constants to be determined. Similarly, one can expand the coefficients A_n, B_n, C_n and D_n into power series:

$$A_m = \sum_{n=0}^{\infty} A_n^{(m)} \bar{S}^n, B_m = \sum_{n=0}^{\infty} B_n^{(m)} \bar{S}^n, C_m = \sum_{n=0}^{\infty} C_n^{(m)} \bar{S}^n, D_m = \sum_{n=0}^{\infty} D_n^{(m)} \bar{S}^n, \tag{31}$$

where the constant coefficients $A_n^{(m)}$, $B_n^{(m)}$, $C_n^{(m)}$ and $D_n^{(m)}$ are known because A_n, B_n, C_n and D_n are known. Note that

$$\bar{u}'' = \sum_{n=2}^{\infty} \bar{u}_n n(n-1)\bar{S}^{n-2} = \sum_{n=0}^{\infty} \bar{u}_{n+2}(n+2)(n+1)\bar{S}^n, \tag{32}$$

$$A_2\bar{u}'' = \left(\sum_{n=0}^{\infty} A_n^{(2)}\bar{S}^n\right)\left(\sum_{n=0}^{\infty} \bar{u}_{n+2}(n+2)(n+1)\bar{S}^n\right)$$
$$= \sum_{n}^{\infty}\left[\sum_{m=0}^{n} A_{n-m}^{(2)}\bar{u}_{m+2}(m+2)(m+1)\right]\bar{S}^n. \tag{33}$$

Therefore, by substituting Eqs. (30) and (31) into Eqs. (26) and (27), we arrive at a pair of algebraic equations for the unknown constants $\bar{u}_n$ and $\bar{v}_n$:

$$P_n + \alpha^2\bar{u}_n = 0, \quad Q_n + \alpha^2\bar{v}_n = 0 \quad \text{for } n = 0, 1, \ldots \infty, \tag{34}$$

where the expressions of P_n and Q_n are given in Appendix C.

Eq. (34) can be solved in a recursive manner, so that all the unknown coefficients $\bar{u}_n$ and $\bar{v}_n$ can be obtained in terms of six constants

$$\mathbf{w} = (\bar{u}_0, \bar{v}_0, \bar{v}_1, \bar{u}_1, \bar{v}_2, \bar{v}_3)^{\mathrm{T}}. \tag{35}$$

To this end, let us first consider $P_0 + \alpha^2\bar{u}_0 = 0$, i.e.,

$$2A_0^{(2)}\bar{u}_2 + A_0^{(1)}\bar{u}_1 + A_0^{(0)}\bar{u}_0 + 6B_0^{(3)}\bar{v}_3 + 2B_0^{(2)}\bar{v}_2 + B_0^{(1)}\bar{v}_1 + B_0^{(0)}\bar{v}_0 + \alpha^2\bar{u}_0 = 0. \tag{36}$$

It can be seen from Appendix B that $A_0^{(2)} \neq 0$. Therefore, $\bar{u}_2$ can be solved from the above in terms of $\mathbf{w}$.

Next, consider

$$P_1 + \alpha^2\bar{u}_1 = 0, \quad Q_0 + \alpha^2\bar{v}_0 = 0. \tag{37}$$

From the expressions of P_n and Q_n it can be seen that Eq. (37) is a pair of equations for $\bar{u}_3$ and $\bar{v}_4$. Also, $P_n + \alpha^2\bar{u}_n = 0$ and $Q_n + \alpha^2\bar{v}_n = 0$ for $n \geqslant 1$ yields a pair of equations for $\bar{u}_{n+2}$ and $\bar{v}_{n+3}$:

$$(n+2)(n+1)A_0^{(2)}\bar{u}_{n+2} + (n+3)(n+2)(n+1)B_0^{(3)}\bar{v}_{n+3} = p_n, \tag{38}$$

$$(n+2)(n+1)nD_0^{(3)}\bar{u}_{n+2} + (n+3)(n+2)(n+1)nC_0^{(4)}\bar{v}_{n+3} = q_{n-1}, \tag{39}$$

where

$$p_n = -\sum_{m=0}^{n-1}\{A_{n-m}^{(2)}\bar{u}_{m+2}(m+2)(m+1) + B_{n-m}^{(3)}\bar{v}_{m+3}(m+3)(m+2)(m+1)\}$$
$$-\sum_{m=0}^{n}\{A_{n-m}^{(1)}\bar{u}_{m+1}(m+1) + A_{n-m}^{(0)}\bar{u}_m + B_{n-m}^{(2)}\bar{v}_{m+2}(m+2)(m+1)$$
$$+ B_{n-m}^{(1)}\bar{v}_{m+1}(m+1) + B_{n-m}^{(0)}\bar{v}_m\} - \alpha^2\bar{u}_n \quad \text{for } n \geqslant 1, \tag{40}$$

$$q_0 = -(2D_0^{(2)}\bar{u}_2 + D_0^{(1)}\bar{u}_1 + D_0^{(0)}\bar{u}_0 + 6C_0^{(3)}\bar{v}_3 + 2C_0^{(2)}\bar{v}_2 + C_0^{(1)}\bar{v}_1 + C_0^{(0)}\bar{v}_0 + \alpha^2\bar{v}_0),$$

$$q_n = -\sum_{m=0}^{n-1}\{D_{n-m}^{(3)}\bar{u}_{m+3}(m+3)(m+2)(m+1) + C_{n-m}^{(4)}\bar{v}_{m+4}(m+4)(m+3)(m+2)(m+1)\}$$
$$-\sum_{m=0}^{n}\{D_{n-m}^{(2)}\bar{u}_{m+2}(m+2)(m+1) + D_{n-m}^{(1)}\bar{u}_{m+1}(m+1) + D_{n-m}^{(0)}\bar{u}_m$$
$$+ C_{n-m}^{(3)}\bar{v}_{m+3}(m+3)(m+2)(m+1) + C_{n-m}^{(2)}\bar{v}_{m+2}(m+2)(m+1)$$
$$+ C_{n-m}^{(1)}\bar{v}_{m+1}(m+1) + C_{n-m}^{(0)}\bar{v}_m\} - \alpha^2\bar{v}_{n-1} \quad \text{for } n \geqslant 1. \tag{41}$$

It is noted that the right-hand sides of Eqs. (38) and (39) contain only terms up to $\bar{u}_{n+1}$ and $\bar{v}_{n+2}$. Furthermore, it is easy to show from the expressions given in Appendix B that

$$K \equiv \begin{vmatrix} A_0^{(2)} & B_0^{(3)} \\ D_0^{(3)} & C_0^{(4)} \end{vmatrix} = -\frac{r^2}{12(1+\varepsilon_0)}\bigg|_{\bar{S}=0} \neq 0. \tag{42}$$

Therefore, $\bar{u}_{n+2}$ and $\bar{v}_{n+3}$ can be solved from Eqs. (38) and (39),

$$\bar{u}_{n+2} = \frac{C_0^{(4)} n p_n - B_0^{(3)} q_{n-1}}{(n+2)(n+1)nK}, \quad \bar{v}_{n+3} = \frac{A_0^{(2)} q_{n-1} - D_0^{(3)} n p_n}{(n+3)(n+2)(n+1)nK}, \quad n \geqslant 1. \tag{43}$$

Once the coefficients $\bar{u}_n$ and $\bar{v}_n$ are obtained, the displacements can be computed from Eq. (30). The coefficients $\bar{u}_n$ and $\bar{v}_n$ depend on the choice of $\mathbf{w} = (\bar{u}_0, \bar{v}_0, \bar{v}_1, \bar{u}_1, \bar{v}_2, \bar{v}_3)^{\mathrm{T}}$. Using $\mathbf{w}^{(1)} = (1,0,0,0,0,0)^{\mathrm{T}}$, $\mathbf{w}^{(2)} = (0,1,0,0,0,0)^{\mathrm{T}}$, etc., one obtains six solutions $\bar{u}^{(k)}$ and $\bar{v}^{(k)}$ ($k = 1, 2, \ldots, 6$), which are also functions of α,

$$\bar{u}^{(k)}(S,\alpha) = \sum_{n=0}^{\infty} \bar{u}_n^{(k)} \bar{S}^n, \quad \bar{v}^{(k)}(S,\alpha) = \sum_{n=0}^{\infty} \bar{v}_n^{(k)} \bar{S}^n. \tag{44}$$

Clearly, we have

$$\bar{u}^{(k)}(0,\alpha) = \delta_{k1}, \quad \bar{v}^{(k)}(0,\alpha) = \delta_{k2}, \quad \frac{\mathrm{d}\bar{v}^{(k)}}{\mathrm{d}S}\bigg|_{S=0} = \delta_{k3}, \tag{45}$$

where δ_{ij} is the Kronecker delta.

The general solution to Eqs. (26) and (27) can then be expressed as

$$\bar{u}(S,\alpha) = \sum_{k=1}^{6} c_k \bar{u}^{(k)}(S,\alpha), \quad \bar{v}(S,\alpha) = \sum_{k=1}^{6} c_k \bar{v}^{(k)}(S,\alpha), \tag{46}$$

where $\mathbf{c} = (c_1, c_2, c_3, c_4, c_5, c_6)^{\mathrm{T}}$ are constants to be determined from the boundary conditions Eq. (29), in conjunction with Eq. (45),

$$\begin{bmatrix} \mathbf{I} & \mathbf{0} \\ \mathbf{F}(\alpha) & \mathbf{G}(\alpha) \end{bmatrix} \mathbf{c} = \mathbf{0}, \tag{47}$$

where $\mathbf{I}$ is a 3×3 identity matrix and

$$\mathbf{F}(\alpha) = \begin{bmatrix} \bar{u}^{(1)}(1,\alpha) & \bar{u}^{(2)}(1,\alpha) & \bar{u}^{(3)}(1,\alpha) \\ \bar{v}^{(1)}(1,\alpha) & \bar{v}^{(2)}(1,\alpha) & \bar{v}^{(3)}(1,\alpha) \\ \dfrac{\mathrm{d}\bar{v}^{(1)}(S,\alpha)}{\mathrm{d}S}\bigg|_{S=1} & \dfrac{\mathrm{d}\bar{v}^{(2)}(S,\alpha)}{\mathrm{d}S}\bigg|_{S=1} & \dfrac{\mathrm{d}\bar{v}^{(3)}(S,\alpha)}{\mathrm{d}S}\bigg|_{S=1} \end{bmatrix}, \tag{48}$$

$$\mathbf{G}(\alpha) = \begin{bmatrix} \bar{u}^{(4)}(1,\alpha) & \bar{u}^{(5)}(1,\alpha) & \bar{u}^{(6)}(1,\alpha) \\ \bar{v}^{(4)}(1,\alpha) & \bar{v}^{(5)}(1,\alpha) & \bar{v}^{(6)}(1,\alpha) \\ \dfrac{\mathrm{d}\bar{v}^{(4)}(S,\alpha)}{\mathrm{d}S}\bigg|_{S=1} & \dfrac{\mathrm{d}\bar{v}^{(5)}(S,\alpha)}{\mathrm{d}S}\bigg|_{S=1} & \dfrac{\mathrm{d}\bar{v}^{(6)}(S,\alpha)}{\mathrm{d}S}\bigg|_{S=1} \end{bmatrix}. \tag{49}$$

In Eq. (47) are six homogeneous equations for a_n. For non-trivial solution, the determinant must vanish, i.e.,

$$D(\alpha) = ||\mathbf{G}(\alpha)|| = 0. \tag{50}$$

Let the roots of the above characteristic equation be α_n. Then, the natural frequencies of the beam are given by Eq. (28),

$$\omega_n = \alpha_n \sqrt{\frac{E}{\rho L^2}}. \tag{51}$$

The corresponding modes are obtained from Eqs. (47) and (46), namely,

$$\bar{u}(S,\alpha_n) = \sum_{k=4}^{6} c_k \bar{u}^{(k)}(S,\alpha_n), \quad \bar{v}(S,\alpha_n) = \sum_{k=4}^{6} c_k \bar{v}^{(k)}(S,\alpha_n), \tag{52}$$

where the constants c_n satisfy

$$\mathbf{G}(\alpha_n)\begin{bmatrix} c_4 \\ c_5 \\ c_6 \end{bmatrix} = \mathbf{0}. \tag{53}$$

5. Numerical examples

In this section, we consider a cantilever beam with prescribed deflection and rotation at its "free" end, see Fig. 1. It is assumed that the initial undeformed beam is a straight beam of length L. Under a concentrated load T, the free end of the beam will come into contact with a fixed rigid surface given by

$$\bar{y} = \bar{x} \tan \theta_f + Y_0, \quad 0 \leqslant \theta_f \leqslant \pi. \tag{54}$$

where θ_f and Y_0 are given parameters to describe the surface. Furthermore, it is assumed that the concentrated force T is, at the final deformed configuration, perpendicular to the surface described by Eq. (54). Note that T is an unknown to be solved from the boundary value problem. To further simplify this problem, we assume that the axial strain in the static deformation is negligible, i.e., $\varepsilon_0 = 0$. This assumption was shown to involve little error [14]. Under these assumptions, the boundary conditions for the statically deformed beam are

$$\theta_0(0) = 0, \quad \theta_0(L) = \theta_f, \tag{55}$$

$$y_0(0) = x_0(0) = 0, \quad y_0(L) = x_0(L) \tan \theta_f + Y_0. \tag{56}$$

The parametric equations of the static deflection curve are

$$x_0(\phi) = L[\hat{x}_0(k,p,\phi) - \hat{x}_0(k,p,\phi_0)], \tag{57}$$

$$y_0(\phi) = L[\hat{y}_0(k,p,\phi) - \hat{y}_0(k,p,\phi_0)], \tag{58}$$

where

$$\hat{x}_0(k,p,\phi) = -\frac{2p}{k} \cos \theta_f \cos \phi + \frac{1}{k} \sin \theta_f [2E(p,\phi) - F(p,\phi)], \tag{59}$$

$$\hat{y}_0(k,p,\phi) = -\frac{1}{k} \cos \theta_f [2E(p,\phi) - F(p,\phi)] - \frac{2p}{k} \sin \theta_f \cos \phi \tag{60}$$

with $F(p,\phi)$ and $E(p,\phi)$ being the elliptical integrals of the first and second kinds, respectively,

$$F(p,\phi) = \int_0^{\phi} \frac{\mathrm{d}z}{\sqrt{1 - p^2 \sin^2 z}}, \quad E(p,\phi) = \int_0^{\phi} \sqrt{1 - p^2 \sin^2 z}\, \mathrm{d}z.$$

The intermediate variable ϕ in the above parametric equations is related to the length variable S through

$$S = \frac{L}{k} \int_{\phi_0}^{\phi} \frac{\mathrm{d}\tau}{\sqrt{1 - p^2 \sin^2 \tau}}, \tag{61}$$

where

$$\phi_0 = \sin^{-1}\left[\frac{\sin(-\theta_f/2 + \pi/4)}{p}\right]. \tag{62}$$

In terms of the Jacobi Amplitude function am(p,q), Eq. (61) can also be written as $\phi = \mathrm{am}(p, kS/p + F(p, \phi_0))$.

The constants k and p in the above equations are determined through the following algebraic equations:

$$k = \int_{\phi_0}^{\phi_L} \frac{1}{\sqrt{1 - p^2 \sin^2 \phi}}\, \mathrm{d}\phi, \tag{63}$$

$$\frac{2}{k}\int_{\phi_0}^{\phi_L} \sqrt{1 - p^2 \sin^2 \tau}\, \mathrm{d}\tau = 1 - \frac{Y_0}{L}\cos\,\theta_f, \tag{64}$$

where

$$\phi_L = \pi - \sin^{-1}\left[\frac{\sin(\pi/4)}{p}\right]. \tag{65}$$

Note that $\tan\,\theta_0 = \mathrm{d}y_0/\mathrm{d}x_0$. It then follows from Eqs. (57) and (58) that

$$\theta_0' = \frac{\mathrm{d}\theta_0}{\mathrm{d}S} = \frac{\mathrm{d}\theta_0}{\mathrm{d}\phi}\frac{\mathrm{d}\phi}{\mathrm{d}S} = \frac{2kp}{L}\cos\,\phi. \tag{66}$$

Higher derivatives θ_0'', θ_0''' and θ_0'''' can thus be obtained analytically as functions of ϕ,

$$\theta_0'' = -\frac{2k^2 p}{L^2}\sin\,\phi\sqrt{1 - p^2\sin^2\phi}, \tag{67}$$

$$\theta_0''' = \frac{2k^3 p}{L^3}\cos\,\phi(2p^2\sin^2\phi - 1), \tag{68}$$

$$\theta_0'''' = \frac{1}{L^4}[2k^4 p(1 + p^2 + 3p^2\,\cos 2\phi)\sin\phi\sqrt{1 - p^2\sin^2\phi}]. \tag{69}$$

Since ϕ is related to S through Eq. (61), one can then evaluate the coefficients given in Appendix A as functions of S.

Numerical examples are conducted for several cases to investigate the effects of the geometrical parameters, Y_0, θ_f and r on the vibration characteristics. The solution procedure consists of:

(1) Compute the static deformation, see [14], to obtain $\theta_0(S)$.
(2) Make use of Eqs. (61)–(69) to compute the derivatives of $\theta_0(S)$ as function of S.
(3) Substitute the known derivatives of $\theta_0(S)$ into the expressions in Appendix B.
(4) Compute the coefficients, $A_n^{(m)}$, $B_n^{(m)}$,$C_n^{(m)}$ and $D_n^{(m)}$. This was done by a curve fitting technique using MatLab ($\varepsilon_0 = 0$ is assumed in the numerical examples presented here).
(5) Substitute these coefficients into Eq. (43) to obtain $\bar{u}_n^{(k)}$ and $\bar{v}_n^{(k)}$ ($k = 1, 2,\ldots,6$) by using six different boundary conditions, $\mathbf{w}^{(1)} = (1,0,0,0,0,0)^{\mathrm{T}}$, $\mathbf{w}^{(2)} = (0,1,0,0,0,0)^{\mathrm{T}}$, ….
(6) Construct the matrix $\mathbf{G}(\alpha)$ according to Eq. (49).
(7) Solve Eq. (50) to obtain the natural frequencies.
(8) Solve Eq. (47) to obtain the corresponding eigenvectors $\mathbf{c}$.
(9) Substitute $\mathbf{c}$ into Eq. (46) to obtain the mode shape.

First, consider that case where $Y_0/L = 0.2$, $r = h/L = 0.06$ and θ_f varies from 0° to 120°. The corresponding first three natural frequencies are shown in Fig. 5. It is seen that the frequencies of the second and third modes approach each other around $\theta_f = 60^\circ$. Very careful examination near that region shows that these two natural frequencies never actually cross each other. But, it can be seen from Figs. 6 and 7,

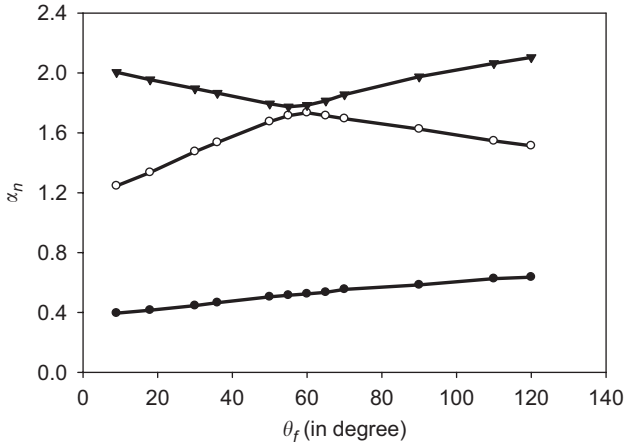

Fig. 5. The first three natural frequencies as a function of θ_f for $Y_0/L = 0.2$, $r = h/L = 0.06$. ●, the first natural frequency; ○, the second natural frequency; and ▼, the third natural frequency.

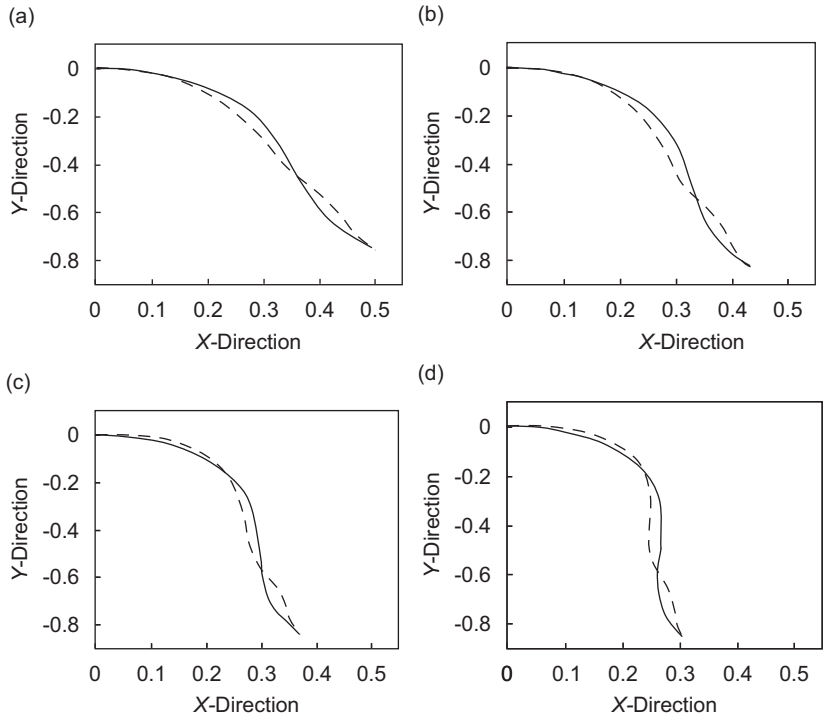

Fig. 6. The second mode of vibration for $Y_0/L = 0.2$, $r = h/L = 0.06$ and (a) $\theta_f = 50^\circ$, (b) $\theta_f = 55^\circ$, (c) $\theta_f = 60^\circ$, and (d) $\theta_f = 65^\circ$. The solid lines are for the initial statically deformed shape, and the dashed lines are the vibration mode shape.

that the corresponding modes do change drastically. The mode corresponding to the second natural frequency has two 'lobes' for $\theta_f < 55^\circ$ and changes to three lobes for $\theta_f > 60^\circ$, while the third mode has three lobes for $\theta_f < 55^\circ$ and changes to two lobes for $\theta_f > 60^\circ$. This is similar to the 'veering' phenomenon discussed in Refs. [15–17].

The effect of Y_0 on the natural frequencies is shown in Fig. 8, where the first three natural frequencies corresponding to $\theta_f = 30^\circ$, $r = h/L = 0.06$ are shown for Y_0/L varying from 0.2 to 0.6. The veering phenomenon discussed in the previous paragraph is also observed here. To see how the beam thickness affects

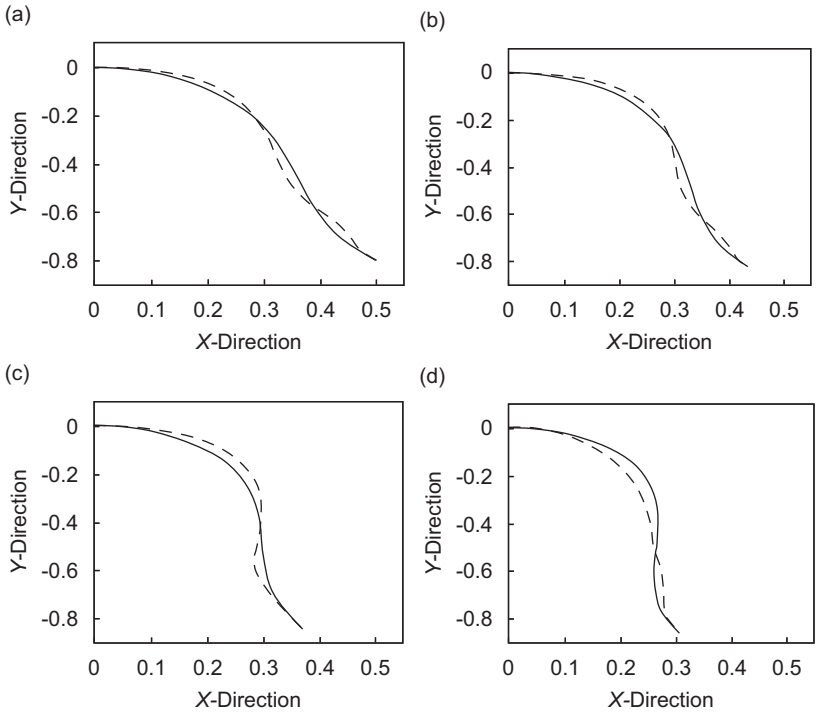

Fig. 7. The third mode of vibration for $Y_0/L = 0.2$, $r = h/L = 0.06$ and (a) $\theta_f = 50^\circ$, (b) $\theta_f = 55^\circ$, (c) $\theta_f = 60^\circ$, and (d) $\theta_f = 65^\circ$. The solid lines are for the initial statically deformed shape, and the dashed lines are the vibration mode shape.

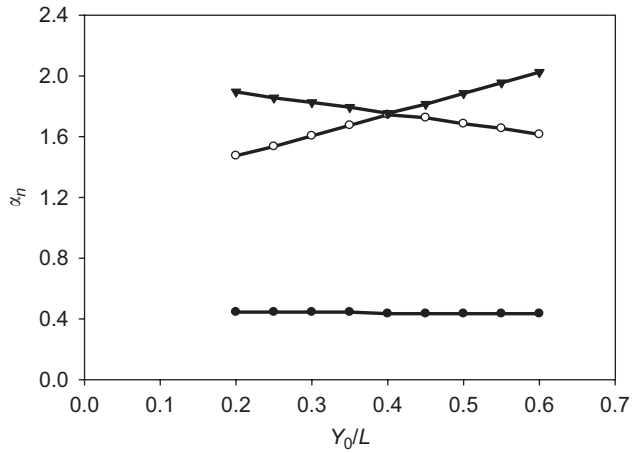

Fig. 8. The first three natural frequencies as function of Y_0/L for $\theta_f = 30^\circ$, $r = h/L = 0.06$. ●, the first natural frequency; ○, the second natural frequency; and ▼, the third natural frequency.

the natural frequencies, numerical solutions for $Y_0/L = 0.2$, $\theta_f = 9^\circ$ were carried out for $r = h/L$ varying from 0.04 to 0.08. The corresponding first three natural frequencies are shown in Fig. 9. As expected, the natural frequencies increase with increasing beam thickness.

An interesting comparison can be made between an initially straight beam that has been deformed by a static force and a beam with initial shape identical to the statically deformed beam. Obviously, the major difference between these two beams is that at the initial state the statically deformed beam has internal stresses, while the naturally curved beam is stress free. The vibration characteristics are certainly affected by the initial stresses. Intuitively, one would expect that the initially stressed beam would have higher natural frequencies.

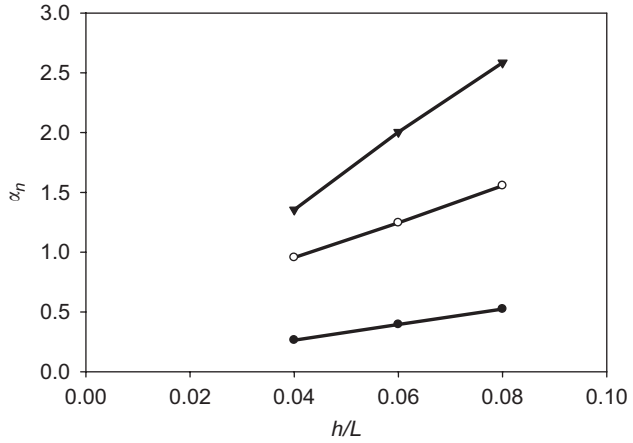

Fig. 9. Natural frequencies as a function of beam thickness: ●, the first natural frequency; ○, second natural frequency; and ▼, the third natural frequency.

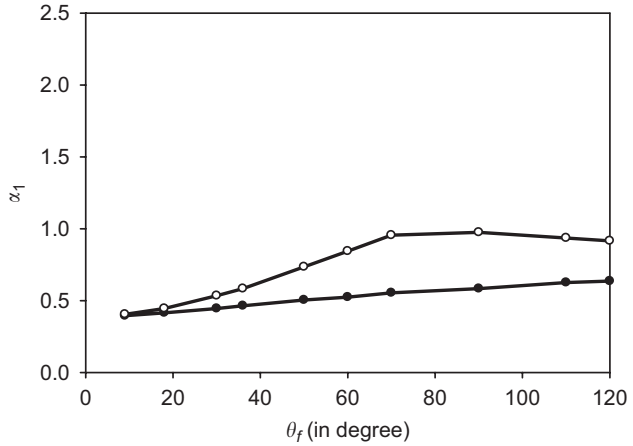

Fig. 10. The first natural frequency of the statically deformed beam (●) and the naturally curved beam (○).

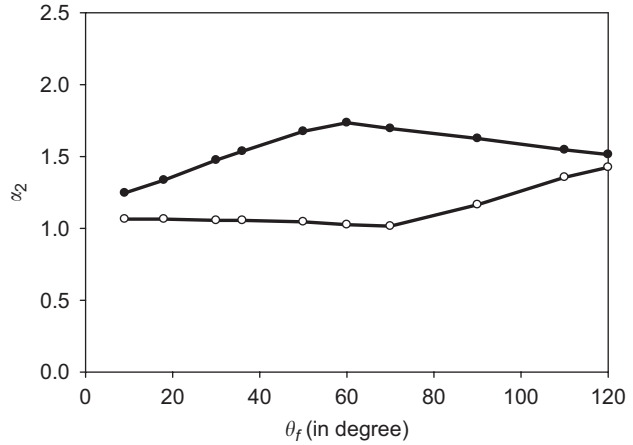

Fig. 11. The second natural frequency of the statically deformed beam (●) and the naturally curved beam (○).

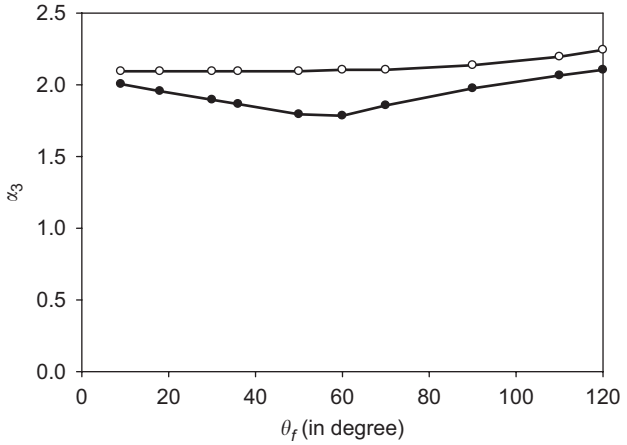

Fig. 12. The third natural frequency of the statically deformed beam (●) and the naturally curved beam (○).

However, from numerical results seem it was concluded that this is not always the case. Shown in Figs. 10–12 are the first three natural frequencies for these two cases for $Y_0/L = 0.2$, $r = h/L = 0.06$ and θ_f varying from 0° to 120°. The boundary conditions used for both types of beams are the same, namely, the "fixed" end ($S = 0$) is rigidly clamped to the vertical wall while the "free" end ($S = L$) is constrained to be touching the inclined surface, but is free to move along the surface. The method used to compute the natural frequencies of such a naturally curved beam was taken from Ref. [18]. It is seen that the frequencies of the naturally curved beams is higher first and third modes are higher, while the frequency of the deformed beams second mode is higher. Although no definitive trend is found, from careful examination of the natural frequency behavior it was found that if the vibration modes of the statistically deformed beam are closer to the static deformation, their natural frequencies tend to be lower. On the other hand, if the vibration modes of the statistically deformed beam are very different from the static deformation, their natural frequencies tend to be higher.

6. Summary and concluding remarks

In this paper, the vibration characteristics of an initially straight beam under large static deflection were investigated. The general equations of motion for a beam subjected to large deflection were derived first. Under the assumption that the amplitude of vibration is much smaller than the static deflection, the nonlinear equations of motion were decomposed into a set of nonlinear differential equations for the static deformation and a set of linear differential equations for the vibration. The coefficients of the linear vibration equations involve the solution to the nonlinear static equation, which were solved by using a method described in Ref. [14]. The linear vibration equation was solved by using the method involving power-series expansions.

Numerical examples were given of cantilever beams subjected to a static concentrated force at the free end. Solutions to the first three natural frequencies and the corresponding vibration modes were presented. The well-known veering phenomenon was found to exist in such beams. Comparison was made between the natural frequencies of the statically deformed beams and the naturally curved beams that have a same initial shape. Intuitively, one would think that the statically deformed beam has been "pre-stressed", and thus may be more "rigid". Consequently, the statically (or pre-stressed) beam may have higher natural frequencies. Our numerical results show that two such beams of the same initial shape do indeed have different natural frequencies. However, it is found that the statically deformed beams may not always have higher natural frequencies. Although there does not seem to be a general trend in whether the statically deformed beam will have higher or lower natural frequencies than a naturally curved beam of the same shape, it seems from the numerical results that for the vibration modes that are closer to the static deformation, their natural frequencies become somewhat lower, while for the vibration modes that are very different from the static deformation, the natural frequencies become higher.

The method developed in this paper for analyzing the vibration of a beam under large static deflection has several advantages. To the authors' knowledge, this is the first attempt to solve such a problem. The solution for the natural frequency involves solving a 3×3 eigenvalue problem. Once the eigenvalue and corresponding eigenvectors are found numerically, the displacements (modes) are given analytically.

Acknowledgments

The authors acknowledge financial support from Visteon. Jianmin Qu was also supported in part by Harbin Institute of Technology through a Guest Professorship.

Appendix A. Displacement equations of motion

Eq. (22) can be converted to

$$x_1 = u\cos\theta_0 - v\sin\theta_0, \quad y_1 = u\sin\theta_0 + v\cos\theta_0. \tag{A.1}$$

It thus follows from Eq. (A.1) that

$$\frac{\mathrm{d}x_1}{\mathrm{d}S} = (u' - v\theta_0')\cos\theta_0 - (u\theta_0' + v')\sin\theta_0, \tag{A.2}$$

$$\frac{\mathrm{d}y_1}{\mathrm{d}S} = (u' - v\theta_0')\sin\theta_0 + (u\theta_0' + v')\cos\theta_0. \tag{A.3}$$

Consequently, it follows from Eq. (8) that

$$\theta_1(1+\varepsilon_0) = -\frac{\mathrm{d}x_1}{\mathrm{d}S}\sin\theta_0 + \frac{\mathrm{d}y_1}{\mathrm{d}S}\cos\theta_0 = u\theta_0' + v' \tag{A.4}$$

and

$$\varepsilon_1 = \frac{\mathrm{d}x_1}{\mathrm{d}S}\cos\theta_0 + \frac{\mathrm{d}y_1}{\mathrm{d}S}\sin\theta_0 = u' - v\theta_0'. \tag{A.5}$$

Note that

$$\rho\left(\frac{\partial^2 x_1}{\partial t^2}\cos\theta_0 + \frac{\partial^2 y_1}{\partial t^2}\sin\theta_0\right) = \rho\frac{\partial^2 u}{\partial t^2}, \quad \rho\left(-\frac{\partial^2 x_1}{\partial t^2}\sin\theta_0 + \frac{\partial^2 y_1}{\partial t^2}\cos\theta_0\right) = \rho\frac{\partial^2 v}{\partial t^2}. \tag{A.6}$$

Therefore, by multiplying Eq. (18) by $\cos\theta_0$ and Eq. (19) by $\sin\theta_0$, and by adding the two equations so modified, one obtains

$$EI\frac{\theta_0'}{1+\varepsilon_0}\theta_1'' - EA\varepsilon_0\theta_0'\theta_1 + EI\left(\frac{\theta_0''\theta_1}{1+\varepsilon_0}\right)' + EA\varepsilon_1' - EI\frac{\theta_0'\theta_0''}{(1+\varepsilon_0)^2}\varepsilon_1 = \rho A\ddot{u}. \tag{A.7}$$

Similarly, by multiplying Eq. (18) by $-\sin\theta_0$ and Eq. (19) by $\cos\theta_0$, and by adding the two equations so modified, one obtains

$$-EI\left(\frac{\theta_1''}{1+\varepsilon_0}\right)' + EA(\varepsilon_0\theta_1)' + EI\frac{\theta_0''\theta_1\theta_0'}{1+\varepsilon_0} + EA\varepsilon_1\theta_0' + EI\left(\frac{\theta_0''\varepsilon_1}{(1+\varepsilon_0)^2}\right)' = \rho A\ddot{v}. \tag{A.8}$$

Substitution of Eqs. (A.4) and (A.5) into Eq. (A.6) yields a second-order ordinary differential equation for u. Similarly, substitution of Eqs. (A.4) and (A.5) into Eq. (A.7) yields a fourth-order ordinary differential equation for v. They are

$$\sum_{n=0}^{2} A_n L^n \frac{\mathrm{d}^n u}{\mathrm{d}S^n} + \sum_{n=0}^{3} B_n L^n \frac{\mathrm{d}^n v}{\mathrm{d}S^n} = \frac{\rho L^2 \ddot{u}}{E}, \tag{A.9}$$

$$\sum_{n=0}^{4} C_n L^n \frac{\mathrm{d}^n v}{\mathrm{d}S^n} + \sum_{n=0}^{3} D_n L^n \frac{\mathrm{d}^n u}{\mathrm{d}S^n} = \frac{\rho L^2 \ddot{v}}{E}, \tag{A.10}$$

where the constants A_n, B_n, C_n and D_n are functions of the static deflection, as well as the geometry and material properties of the beam. Their expressions are given in Appendix B.

Appendix B. Expressions for A_n, B_n, C_n and D_n

$$A_2 = 1 + \frac{r^2 L^2}{12}\left(\frac{\theta_0'}{1+\varepsilon_0}\right)^2, \tag{B.1}$$

$$A_1 = \frac{L^3 r^2}{12}\left[\left(\frac{\theta_0'}{1+\varepsilon_0}\right)^2\right]' = \frac{L^3 r^2 \theta_0'}{6(1+\varepsilon_0)^2}\left[\theta_0'' - \frac{\theta_0'\varepsilon_0'}{(1+\varepsilon_0)}\right], \tag{B.2}$$

$$\begin{aligned} A_0 = & -L^2\frac{(\theta_0')^2\varepsilon_0}{1+\varepsilon_0} + \frac{L^4 r^2}{12}\frac{\theta_0'}{1+\varepsilon_0}\left(\frac{\theta_0'}{1+\varepsilon_0}\right)'' + \frac{L^4 r^2}{12}\left(\frac{\theta_0'\theta_0''}{(1+\varepsilon_0)^2}\right)' \\ = & \frac{L^4 r^2(\varepsilon_0'\theta_0')^2}{6(1+\varepsilon_0)^4} - \frac{L^4 r^2\theta_0'(\theta_0'\varepsilon_0'' + 4\varepsilon_0'\theta_0'')}{12(1+\varepsilon_0)^3} + \frac{L^4 r^2\left[(\theta_0'')^2 + 2\theta_0'\theta_0'''\right]}{12(1+\varepsilon_0)^2} - \frac{L^2(\theta_0')^2\varepsilon_0}{1+\varepsilon_0}, \end{aligned} \tag{B.3}$$

$$B_3 = \frac{L r^2 \theta_0'}{12(1+\varepsilon_0)^2}, \tag{B.4}$$

$$B_2 = \frac{-L^2 r^2 \varepsilon_0'\theta_0'}{6(1+\varepsilon_0)^3} + \frac{L^2 r^2 \theta_0''}{12(1+\varepsilon_0)^2}, \tag{B.5}$$

$$B_1 = \frac{L^3 r^2(\varepsilon_0')^2\theta_0'}{6(1+\varepsilon_0)^4} - \frac{L^3 r^2(\varepsilon_0''\theta_0' + 2\varepsilon_0'\theta_0'')}{12(1+\varepsilon_0)^3} + \frac{L^3 r^2\theta_0'''}{12(1+\varepsilon_0)^2} - \frac{L(1+2\varepsilon_0)\theta_0'}{1+\varepsilon_0}, \tag{B.6}$$

$$B_0 = -L^2\theta_0'' + \frac{L^4 r^2}{12}\frac{(\theta_0')^2\theta_0''}{(1+\varepsilon_0)^2}, \tag{B.7}$$

$$C_4 = -\frac{r^2}{12(1+\varepsilon_0)^2}, \tag{B.8}$$

$$C_3 = \frac{L r^2 \varepsilon_0'}{3(1+\varepsilon_0)^3}, \tag{B.9}$$

$$C_2 = \frac{\varepsilon_0}{1+\varepsilon_0} + \frac{r^2 L^2}{12(1+\varepsilon_0)^4}[3(1+\varepsilon_0)\varepsilon_0'' - 8(\varepsilon_0')^2], \tag{B.10}$$

$$C_1 = \frac{2L^3 r^2(\varepsilon_0')^3}{3(1+\varepsilon_0)^5} - \frac{7L^3 r^2\varepsilon_0'\varepsilon_0''}{12(1+\varepsilon_0)^4} + \frac{L^3 r^2\varepsilon_0'''}{12(1+\varepsilon_0)^3} + \frac{L\varepsilon_0'}{(1+\varepsilon_0)^2}, \tag{B.11}$$

$$C_0 = \frac{L^4 r^2\varepsilon_0'\theta_0'\theta_0''}{6(1+\varepsilon_0)^3} - \frac{L^4 r^2[(\theta_0'')^2 + \theta_0'\theta_0''']}{12(1+\varepsilon_0)^2} - L^2(\theta_0')^2, \tag{B.12}$$

$$D_3 = \frac{-L r^2 \theta_0'}{12(1+\varepsilon_0)^2}, \tag{B.13}$$

$$D_2 = \frac{r^2L^2\varepsilon_0'\theta_0'}{3(1+\varepsilon_0)^3} - \frac{r^2L^2\theta_0''}{6(1+\varepsilon_0)^2}, \tag{B.14}$$

$$D_1 = -\frac{2L^3r^2(\varepsilon_0')^2\theta_0'}{3(1+\varepsilon_0)^4} + \frac{L^3r^2(\theta_0'\varepsilon_0'' + 2\theta_0''\varepsilon_0')}{4(1+\varepsilon_0)^3} - \frac{L^3r^2\theta_0'''}{6(1+\varepsilon_0)^2} + \frac{L(1+2\varepsilon_0)\theta_0'}{1+\varepsilon_0}, \tag{B.15}$$

$$\begin{aligned} D_0 = {} & \frac{2L^4r^2(\varepsilon_0')^3\theta_0'}{3(1+\varepsilon_0)^5} - \frac{L^4r^2\varepsilon_0'(7\theta_0'\varepsilon_0'' + 8\varepsilon_0'\theta_0'')}{12(1+\varepsilon_0)^4} + \frac{L^4r^2(\varepsilon_0'''\theta_0' + 3\varepsilon_0''\theta_0'' + 4\varepsilon_0'\theta_0''')}{12(1+\varepsilon_0)^3} \\ & + \frac{L^4r^2[(\theta_0')^2\theta_0'' - \theta_0^{(4)}] + 12L^2\varepsilon_0'\theta_0'}{12(1+\varepsilon_0)^2} + \frac{L^2\varepsilon_0\theta_0''}{1+\varepsilon_0}. \end{aligned} \tag{B.16}$$

In the above,

$$r = \frac{h}{L}. \tag{B.17}$$

Appendix C. Expressions of P_n and Q_n

$$\begin{aligned} P_n = \sum_{m=0}^{n} \{ & A_{n-m}^{(2)}\bar{u}_{m+2}(m+2)(m+1) + A_{n-m}^{(1)}\bar{u}_{m+1}(m+1) + A_{n-m}^{(0)}\bar{u}_m \\ & + B_{n-m}^{(3)}\bar{v}_{m+3}(m+3)(m+2)(m+1) + B_{n-m}^{(2)}\bar{v}_{m+2}(m+2)(m+1) \\ & + B_{n-m}^{(1)}\bar{v}_{m+1}(m+1) + B_{n-m}^{(0)}\bar{v}_m \}, \end{aligned} \tag{C.1}$$

$$\begin{aligned} Q_n = \sum_{m=0}^{n} \{ & D_{n-m}^{(3)}\bar{u}_{m+3}(m+3)(m+2)(m+1) + D_{n-m}^{(2)}\bar{u}_{m+2}(m+2)(m+1) \\ & + D_{n-m}^{(1)}\bar{u}_{m+1}(m+1) + D_{n-m}^{(0)}\bar{u}_m + C_{n-m}^{(4)}\bar{v}_{m+4}(m+4)(m+3)(m+2)(m+1) \\ & + C_{n-m}^{(3)}\bar{v}_{m+3}(m+3)(m+2)(m+1) + C_{n-m}^{(2)}\bar{v}_{m+2}(m+2)(m+1) \\ & + C_{n-m}^{(1)}\bar{v}_{m+1}(m+1) + C_{n-m}^{(0)}\bar{v}_m \}. \end{aligned} \tag{C.2}$$

References

[1] S. Crum, Flex circuit materials meet application requirements, *Electronic Packaging Proceeding* 37 (1997) 5–9.

[2] L. Freitag, J. Kuczynski, P. Fortier, F. Guindon, M. Letourneau, B. Chan, J. Sherman, G. Johnson, D. Demangone, M. Mentzer, D. Naghski, B. Trostle, Packaging aspects of the litebus parallel optoelectronic module, *Proceedings of the 50th Electronic Components and Technology Conference*, May 21–24, 2000, Las Vegas, NV, pp. 1259–1265.

[3] H. Isaak, P. Uka, Development of flex stackable carriers, *Proceedings of the 50th Electronic Components and Technology Conference*, May 21–24, 2000, Las Vegas, NV, pp. 378–384.

[4] G. Kirchhoff, On the equilibrium and motion of an infinite thin beam, *Journal of Pure and Applied Mathematics* 56 (1859) 285–290 (in German).

[5] S. Chen, In-plane vibration of continuous curved beams, *Nuclear and Engineering Design* 25 (1973) 413–431.

[6] M. Petyt, C. Fleischer, Free vibration of a curved beam, *Journal of Sound and Vibration* 18 (1971) 17–30.

[7] S. Markus, T. Nanasi, Vibration of curved beams, *Shock Vibration Digest* 13 (1981) 3–14.

[8] K. Suzuki, H. Ishiyama, In-plane vibrations of curved bars, *Bulletin of the Japan Society Mechanical Engineering* 21 (1987) 618–627.

[9] P. Laura, M. Maurizi, Recent research on vibrations of arch-type structures, *Shock Vibration Digest* 19 (1987) 6–9.

[10] P. Chidamparam, A. Leissa, Vibrations of planar curved beams, rings and arches, *Applied Mechanics Reviews* 46 (1993) 467–483.

[11] T. Tarnopolskaya, F.R. de Hoog, A. Tarnopolsky, N.H. Fletcher, Vibrations of beams and helices with arbitrarily large uniform curvature, *Journal of Sound and Vibration* 228 (1999) 305–332.

[12] Y.P. Tseng, C. Lin, Dynamic stiffness analysis for in-plane vibrations of arches with variable curvature, *Journal of Sound and Vibration* 207 (1997) 15–31.

[13] Y.P. Tseng, M. Kao, In-plane vibration of laminated curved beams with variable curvature by dynamic stiffness analysis, *Composite Structures* 50 (2000) 103–114.
[14] Y. Xue, V.A. Jairazhboy, J. Qu, Large deflection of thin plates under certain fixed boundary conditions—cylindrical bending, *Journal of Electronic Packaging* 125 (2003) 53–58.
[15] P. Chen, J. Ginsberg, On the relationship between veering of eigenvalue loci and parameter sensitivity of eigenfunctions, *Journal of Vibration and Acoustics* 114 (1992) 141–148.
[16] A.W. Leissa, The free vibration of rectangular plates, *Journal of Sound and Vibration* 31 (1973) 257–293.
[17] T. Tarnopolskaya, F.R. de Hoog, N.H. Fletcher, Low frequency mode transition in the free in-plane vibration of curved beams, *Journal of Sound and Vibration* 228 (1999) 69–90.
[18] B. Lee, J. Wilson, Free vibrations of arches with variable curvature, *Journal of Sound and Vibration* 6 (1989) 75–89.